Fibrous growth of tricalcium phosphate ceramics

J. J. PRIETO VALDÉS, J. ORTIZ LÓPEZ, G. RUEDA MORALES, G. PACHECO MALAGON
ESFM, Instituto Politécnico Nacional. U.P. Adolfo López Matéos, Edif. 9, México D.F., 07738
V. PRIETO GORTCHEVA
Depto. de Física, CINVESTAV-IPN, Ave. IPN 2508, México D.F., 07300

Structural transformation and sintering processes of tricalcium phosphate (TCP) ceramics prepared from defective hydroxyapatite ($Ca_9HPO_4(PO_4)_5OH$) were studied by X-ray diffraction (XRD) and atomic force microscopy (AFM). Starting powders with Ca/P ratio ~ 1.5 were obtained by adding 0.5 ℓ of 0.3 M H_3PO_4 solution to an equal volume of 0.45 M $Ca(OH)_2$. In the prepared ceramics, the onset temperature for transformation of defective hydroxyapatite into TCP (witlokite) agrees with the onset temperature for sintering (800 °C). Sintering occurs through the formation of a fibrous structure, which resembles biological hard tissue. In the 1000–1200 °C range, these fibres coalesce into grains of up to 0.6 μm in size with a fibrous-laminar morphology. At the end of this sintering stage witlokite transforms into αTCP. At about 1450 °C, partial decomposition of αTCP into $Ca_2P_2O_7 + Ca_4P_2O_9$ is observed. AFM observations suggest that $Ca_2P_2O_7$ is segregated in the liquid state and increases the velocity of grain growth (up to 12 μm).

1. Introduction

The current use of calcium phosphate ceramics in medicine is very common. Hydroxyapatite ($Ca_{10}(PO_4)_6(OH)_2$; HA) and tricalcium phosphate ($Ca_3(PO_4)_2$; TCP) ceramics are among the most widely used due to their biocompatibility [1, 2]. There have been many studies of the behaviour of these ceramics as bone implants [3–8] which consider the morphology as well as the calcium/phosphorous (Ca/P) relative content and structural composition of the material as very important aspects. Published studies about the characteristics and sintering processes of calcium phosphate compounds apply traditional techniques [9–16] such as X-ray diffraction (XRD), infrared spectroscopy, transmission (TEM) and scanning electron microscopy (SEM) as well as analysis of their mechanical properties. In this work we study sintering of TCP by XRD and atomic force microscopy (AFM), paying particular attention to the process of ceramic structural formation and surface morphology.

2. Materials and methods

Starting powders with a Ca/P ratio of $\simeq 1.5$ were obtained by adding 0.5 ℓ of 0.3 M H_3PO_4 solution to an equal volume of 0.45 M $Ca(OH)_2$ suspension. The addition was performed by dripping at 6 ml/min and stirring at constant temperature (40 °C). The resulting compound precipitated after 24 h (under Mexico City altitude conditions) and was then washed with distilled water and dried at 80–90 °C. The powder with $\sim 20\%$ humidity was then ground manually in an agate mortar and pressed into pellets at 100 kg/cm^2 with a 15.25 mm diameter cylindrical die. Prepared pellets had 2 mm thickness and weighed approximately 0.5 g. After pressing, the pellets were dried at 90–100 °C. The pellets were then thermally treated in dry atmosphere by heating from room temperature to 1450 °C at a rate of 5 °C/min. Starting from 700 °C and for each incremental temperature of 50 °C, different samples were extracted from the furnace and quenched in air to study the degree of structural transformation attained during different stages of the sintering process. A great number of pellets were studied in this way in order to statistically test the reproducibility of experimental results. Samples extracted from the furnace after reaching 1450 °C were cooled in two different ways: (a) by quenching, and (b) by slow cooling inside the furnace after switching it off. Finally, a control group of samples were annealed for 30 min at 1450 °C and quenched in air.

The extracted samples were analysed by XRD in a SIEMENS 500 diffractometer using Ni filtered

This paper was accepted for publication after the 1995 Conference of the European Society of Biomaterials, Oporto, Portugal, 10–13 September.

CuK_α radiation at 30 kV and 20 mA. The 2θ angle was swept from 20° to 80° at a rate of 0.1°/min. The surface structure of the samples analysed by XRD were also studied with a Park Scientific Instruments Autoprobe CP atomic force microscope (AFM). For AFM the samples were not specially prepared and were kept in an oven at 100 °C between analyses to avoid surface hydration effects.

3. Result and discussion

3.1. Structural transformation studied by XRD

Fig. 1 shows X-ray diffraction patterns of the studied pellets. The first pattern (after drying at 100 °C) corresponds to the synthesized and pressed powders. All peaks that correspond to synthetic HA are observed (ASTM card N. 9432). The peaks in this pattern are very diffuse and show in some cases a slight displacement which can be explained [13–15] to be due to the formation of poorly crystallized defective HA with Ca/P ratio ~1.5 and to the high dispersion of the powders. As is well known [13], during the reaction of Ca and P carriers under appropriate conditions (Ca/P ratio, pH, temperature, time and pressure), defective HA [$Ca_9HPO_4(PO_4)_5OH$] can be produced. Defective HA and stoichiometric HA have similar crystalline structure with the same space group (P63/m) and their X-ray patterns are very similar.

In Fig. 1, X-ray patterns are also shown of pellets quenched in air after reaching 800 °C and 1100 °C. In the first case (800 °C) peaks characteristic of synthetic witlokite (TCP) are observed (ASTM card N. 9169)

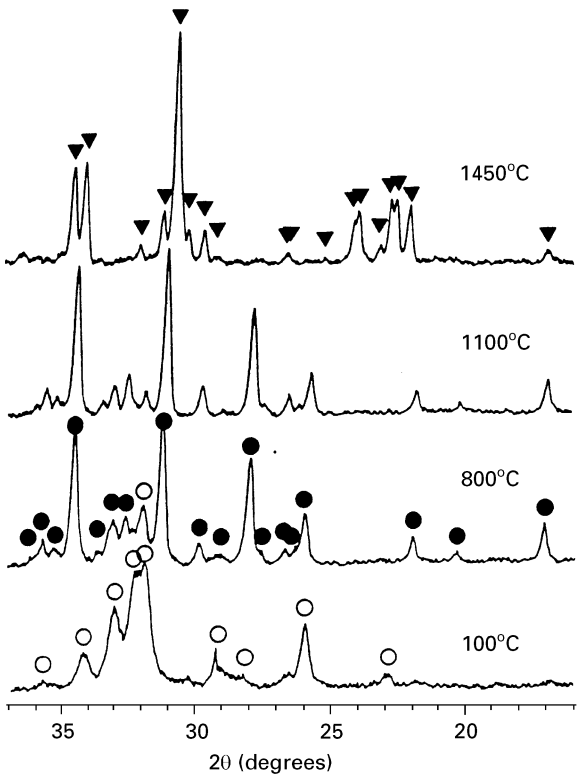

Figure 1 XRD patterns of the quenched pellets after reaching the indicated temperatures O–HA (ASTM card N. 9432), ●–TCP (N. 9169) and ▼–αTCP (N. 9348).

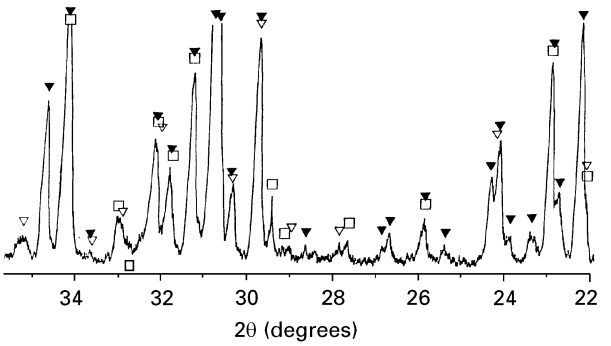

Figure 2 XRD patterns of the sample annealed for 30 min at 1450 °C and quenched in air. ▼–αTCP (ASTM card N. 9348), □–$Ca_4P_2O_9$ (ASTM card N. 11232) and ▽–$Ca_2P_2O_7$ (ASTM card 20647).

and the more intense peaks of HA are still observed. In the second case (1100 °C) peaks corresponding to TCP are better defined and those of HA tend to disappear. Formation of TCP from defective HA must occur in the interval 750–1200 °C through the following reaction:

$$Ca_9(HPO_4)(PO_4)_5(OH) \Rightarrow 3Ca_3(PO_4)_2 + H_2O \quad (1)$$

Finally, the X-ray pattern of samples quenched in air after reaching 1450 °C show that these samples are single phase since in the X-ray patterns only the characteristic peaks of αTCP are observed (ASTM card N. 9348).

Fig. 2 shows the pattern of samples annealed for 30 min at 1450 °C and quenched in air. The patterns of these samples are more complex, and show peaks corresponding to αTCP and other small reflections. These patterns appear slightly distorted with several peaks showing some loss of symmetry and slight displacements which could be attributed to a highly stressed state of the quenched ceramic material and to small concentrations of two other phases. Weak reflections are observed that can be associated with the presence of calcium pyrophosphate ($Ca_2P_2O_7$; ASTM card 20647) and tetracalcium phosphate ($Ca_4P_2O_9$; ASTM card N. 11232). The presence of pyrophosphate and tetracalcium phosphate is understable if we consider the possibility of αTCP (with approximate Ca/P ratio 1.5) partial dissociation at high temperature so that the process of αTCP dissociation is more advanced in samples annealed for 30 min at 1450 °C than in the case of samples quenched after reaching this temperature. Decomposition of αTCP can be explained by the following reaction:

$$2Ca_3(PO_4)_2 \Rightarrow Ca_2P_2O_7 + Ca_4P_2O_9 \quad (2)$$

According to the phase diagram [16], $Ca_2P_2O_7$ melts at approximately 1360 °C so that transformation (2) from non-stoichiometric αTCP must be considered an important fact to take into account in TCP sintering technology.

3.2. AFM structural morphology studies

Only samples treated at temperatures above 800 °C were suitable for atomic force microscopic analysis. Samples treated at lower temperatures did not have

the right surface consistency for good imaging because unbound particles on their surface were subject to drag by the AFM tip. This difficulty indicates that sintering does not take place below 800 °C. In fact, the temperature for the transformation of defective HA into TCP according to reaction (1), agrees with the onset temperature for sintering. This agreement can be attributed to atomic diffusive activity during the phase transformation which in turn activates the sintering process.

Fig. 3 shows an AFM image of the surface of a ceramic sample quenched after an 800 °C thermal treatment. Particles of 0.18 μm average diameter or less are observed, with early bonds forming between each other with a coordination number that varies between 4 and 5 at the surface level. In Fig. 4 a section of a sample quenched after a 1000 °C treatment is shown. Around a micropore, particles with a fibrous morphology (asparagus like) can be seen, having diameters close to those observed for particles in the previous stage of sintering (Fig. 3). Fig. 5 shows a sample quenched after 1100 °C treatment. This image corresponds to the central zone of the surface of the pellet. With increasing temperature we can see that the "primary asparagus" of Fig. 4 coalesce to form a "secondary asparagus" structure. The average diameter of the secondary asparagus reach values of 0.5 μm.

Fig. 6a and 6b show views around two different micropores of samples quenched after heating to 1100 °C. These micropores are observed on the periphery of the ceramic pellet. Now the secondary asparagus are sintered and lose their roundness but the fibrous structure prevails, with rectangular and triangular formations. Fusion of the secondary asparagus induce growth of the ceramic structure grains with

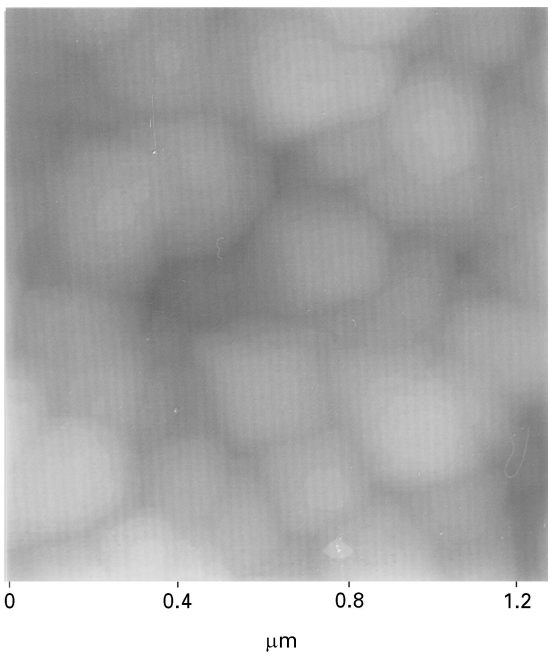

Figure 3 AFM image of the central part of a ceramic pellet quenched in air after reaching 800 °C (this image corresponds to the beginning of the sintering process).

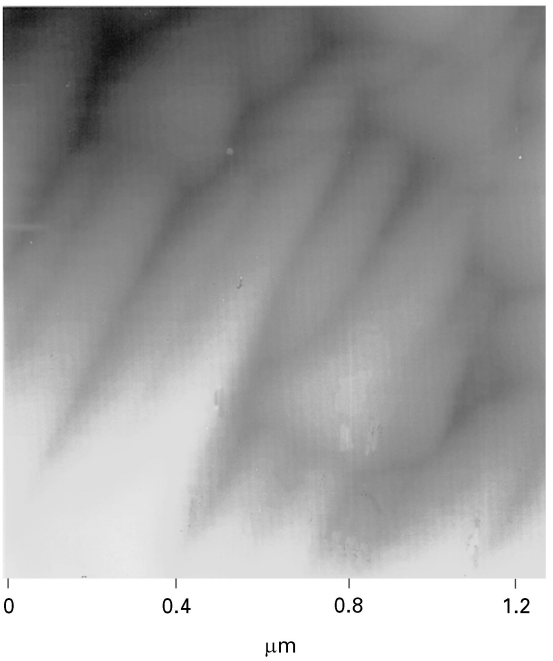

Figure 4 AFM image of the central part of a sample quenched in air after reaching 1000 °C (the formation of "primary asparagus" morphology is observed).

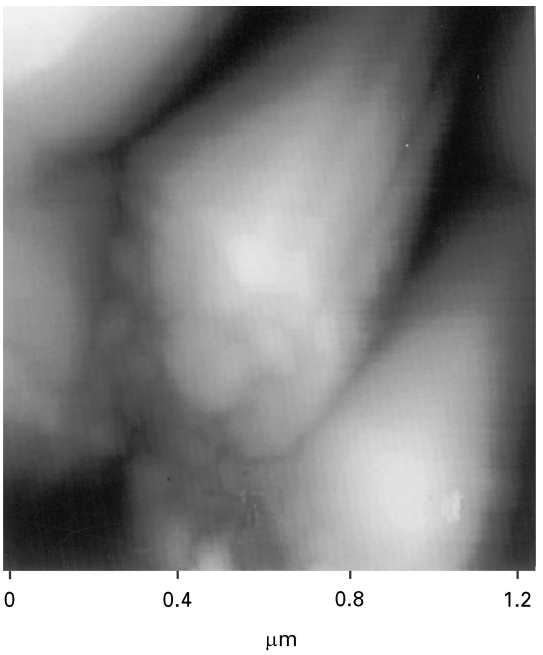

Figure 5 Image of the central part of pellet quenched in air after reaching 1100 °C (the formation of "secondary asparagus" morphology is observed).

sizes up to 0.6 μm. In the lower part of Fig. 6a a coordination number between 6 and 7 can be seen in this secondary asparagus structure.

Fig. 7 shows a 3-D view of the surface of a ceramic quenched after reaching 1450 °C. Formation of large grains are seen that have average sizes between 4 and 6 μm along the edges. The fibrous structure is clearly seen accompanied by small grains that can be identified as small droplets of a liquid phase frozen during

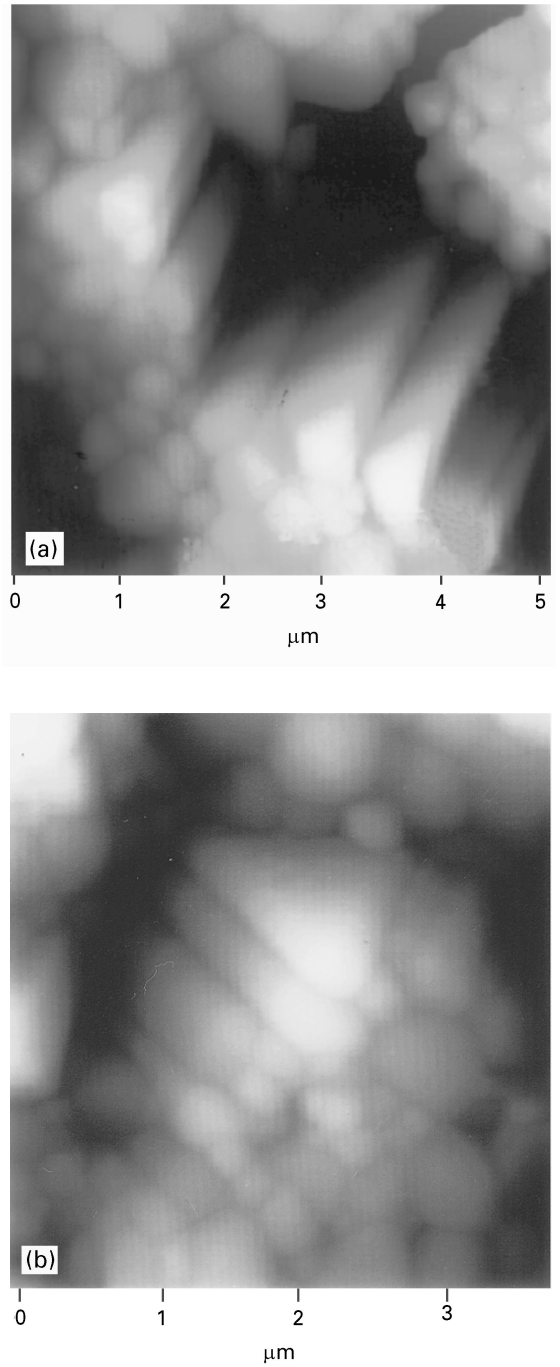

Figure 6 AFM images of two pores (a and b) observed in the periphery of a ceramic sample quenched in air after reaching 1100 °C (the secondary asparagus coalesce giving rise to rectangular and triangular formations).

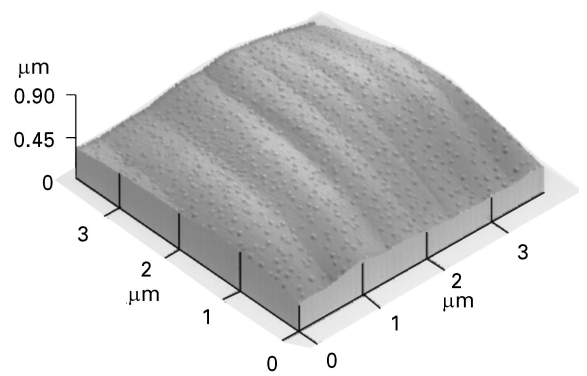

Figure 7 Three-dimensional view of the surface of a ceramic quenched in air after reaching 1450 °C (small droplets of a liquid phase frozen during quenching are observed).

quenching. This can be correlated to the X-ray results for this sample (Fig. 2) where diffuse peaks corresponding to calcium pyrophosphate were detected. As explained at the end of section 3.1, according to the equilibrium phase diagram this pyrophosphate should segregate in its liquid state.

Fig. 8 shows the surface of a ceramic annealed by slow cooling inside the furnace after reaching 1450 °C. Two perpendicular orientations of the fibrous structure can be seen for two neighbouring grains that were arbitrarily chosen.

Fig. 9 is a 3-D view of an amplification of the area at the centre-right of the image shown in Fig. 8. In this sample no signs of solidified droplets can be seen but a very fine fibrous texture is observed, as if the liquid phase that was formed at high temperature had drifted along the surface adopting a fine fibrous structure in the direction of the fibres of the ceramic matrix.

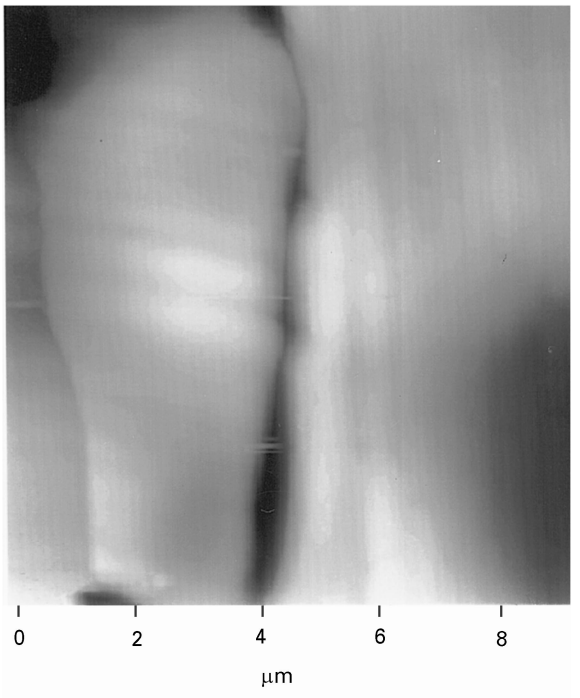

Figure 8 AFM image of a ceramic sample annealed by slow cooling inside the furnace after reaching 1450 °C (larger grains with fibrous structure are observed).

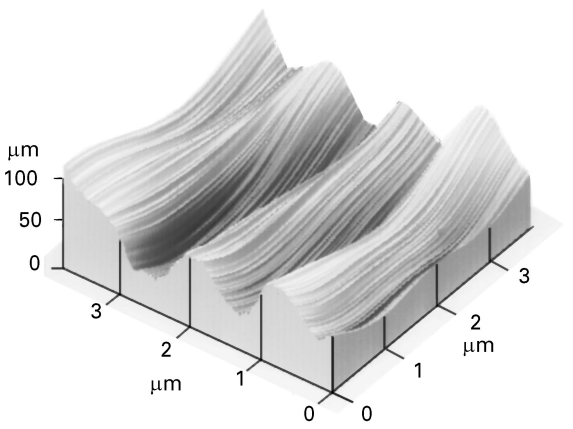

Figure 9 Three-dimensional view of the central right zone of the image shown in Fig. 8.

In general terms, it can be observed that tricalcium phosphate ceramics (with Ca/P $\sim$ 1.5) sintered from synthetic defective hydroxyapatite powders have a fibrous morphology which surprisingly resembles biological hard tissue.

4. Conclusions

1. TCP ceramics sintered from defective HA powders with Ca/P ratio $\sim$1.5 have fibrous morphology. This morphology resembles biological hard tissue.
2. In this type of ceramic, the onset temperature for the transformation of defective HA into TCP (800 °C) agrees with the onset temperature for sintering. This agreement can be attributed to atomic diffusive activity during the phase transformation which in turn activates the sintering process.
3. At about 1450 °C in this type of ceramic, a partial decomposition of αTCP into $Ca_2P_2O_7 + Ca_4P_2O_9$ is observed.
4. AFM observations suggest that $Ca_2P_2O_7$ is segregated in a liquid state and increases the velocity of grain growth (up to 12 μm) in the TCP ceramic matrix.

References

1. K. DE GROOT, *Biomaterials* **1** (1980) 47.
2. M. JARCHO, *Clin. Orthop.* **157** (1981) 259.
3. A. M. GATTI, D. ZAFFE and G. P. POLI, *Biomaterials* **11** (1990) 513.
4. C. P. A. T. KLEIN, A. A. DRIESSEN, K. DE GROOT and A. VAN DEN HOFF, *J. Biomed. Mater Res.* **17** (1983) 769.
5. C. REY, *Biomaterials* **11** (1990) 13.
6. K. HYAKUNA, T. YAMAMURO, Y. KOTOURA, M. OKA, T. NAKAMURA, T. KITSUGI and T. KOKUBO, *J. Biomed. Mater Res.* **24** (1990) 471.
7. P. FRAYSSINET, J. L. TROUILLET, N. ROUQUET, E. AZIMUS and A. ANTEFAGE, *Biomaterials* **14** (1993) 423.
8. K. SHIMAZAKI and V. MOONEY, *J. Orthop. Res.* **3** (1985) 301.
9. K. KIESWETTER, T. W. BAUER, S. A. BROWN, F. VAN LENTE and K. MERRITT, *Biomaterials* **15** (1994) 183.
10. E. PAUCHIU and T. K. CHAKI, *J. Mater. Sci. Mater. Med.* **4** (1993) 150.
11. A. ROYER and J. C. VIGUIE, *ibid.* **4** (1993) 76.
12. M. Y. SHAREEF and P. M. MESSER, *Biomaterials* **14** (1993) 69.
13. F. C. M. DRIESSENS, in "Bioceramics of calcium phosphate", edited by K. de Groot (CRC Press I. Boca Raton, FI, 1983).
14. K. ISHIKAWA, P. DUCHEYNE and S. RADIN, *J. Mater. Sci. Mater. Med.* **4** (1993) 165.
15. J. ZHOU, X. ZHANG, J. CHEN, S. ZENG and K. DE GROOT, *ibid.* **4** (1993) 83.
16. J. H. WELCH and W. GUTT, *J. Chem. Soc.* **874** (1961) 4442; W. L. HILL, G. T. FAUST and D. S. REYNOLDS, *Amer. J. Sci.* **242** (1994) 470.